Investigation of Shear Failure Mechanisms of Pressure-Sensitive Adhesives

FRANCK SOSSON, ANTOINE CHATEAUMINOIS, COSTANTINO CRETON

Laboratoire de Physico-Chimie des Polymères et de la Matière Divisée, UMR CNRS 7615, Ecole Supérieure de Physique et Chimie industrielles (ESPCI), 10 rue Vauquelin, 75231 Paris, Cedex 5, France

Received 7 January 2004; revised 25 August 2005; accepted 25 August 2005
DOI: 10.1002/polb.20619
Published online in Wiley InterScience (www.interscience.wiley.com).

ABSTRACT: We report new experiments investigating the failure mechanisms in shear, of thin layers of acrylic pressure-sensitive adhesives (PSA). We have developed a novel experimental device able to shear a soft adhesive layer confined between a rigid hemispherical lens and a rigid glass substrate. Using the resources of *in situ* contact visualization, the nonhomogeneous deformation of the layer and the shear failure processes were observed optically. Depending on the rheological properties of the adhesive, ratios of the contact radius over the layer thickness of 10–30 were achieved, mimicking well the contact conditions encountered in a thin adhesive layer within a joint. When the adhesive was weakly crosslinked, we observed a fluid-like behavior and could measure a reasonable value for the viscosity of the PSA, implying that flow can occur in the layer and failure will occur by creep. On the other hand, for a more crosslinked adhesive, closer to what is used in applications, a stick-slip peeling behavior was observed, which involves a coupling between peeling mechanisms at the leading edge of the contact and interfacial slippage. Such a process suggests a failure by fracture rather than by creep. Interestingly, the peeling mechanisms and the associated stress levels change significantly when the layer becomes as thin as 20 μm, implying a fracture process that is controlled by a critical energy release rate in shear G_{IIc} rather than by a critical shear stress causing failure of the interfacial bonds. J Polym Sci Part B: Polym Phys 43: 3316–3330, 2005
Keywords: crosslinking; friction; peeling; pressure-sensitive adhesives; shear; viscoelasticity

INTRODUCTION

Polymers are widely used as base materials for the design of adhesives. Their mechanical properties and easy processing makes them ideal candidates for those applications. Among the different classes of adhesives, self-adhesives, otherwise known as pressure-sensitive adhesives (PSA), are based on polymers that are well above their glass-transition temperature and rely on a careful tuning of the rheological properties of the formulated adhesive to function properly.[1]

Permanent PSA are used as thin layers (20–100 μm), which function as adhesive joints and work essentially in shear. Yet, their adhesive properties have almost exclusively been studied with methods applying tension rather than shear, that is, peel tests rather than probe tests.

Industrially, resistance to shear is generally tested with a very simple test, that is, a simple dead load is applied on a standardized area of

Correspondence to: A. Chateauminois
(E-mail: antoine.chateauminois@espci.fr)

Journal of Polymer Science: Part B: Polymer Physics, Vol. 43, 3316–3330 (2005)

adhesive and the time-to-failure is monitored to assess shear resistance (PSTC method 107).[2] While being close to application requirements, this test does not provide any insights on the failure mechanisms of the adhesive layer, and in particular, on the initiation of failure under shear stresses.

Some studies have tried to predict the time-to-failure from the rheological properties of the PSA, as measured in a rheometer.[3] While this approach works well when the adhesive fails cohesively and the shear test can be assimilated to a creep test, it fails miserably to predict the time to interfacial failure. Unfortunately, most commercial PSA are lightly crosslinked and do fail with a mixture of interfacial and cohesive failure, making it necessary to perform long and costly shear tests to evaluate the long-term (up to 10,000 h) performance of the adhesive. Alternative tests based on a precise monitoring of the displacement of the adhesive under stress as a function of time have been reported by industries,[4] but no academic study has so far focused on the failure mechanisms of these soft layers in shear.

On the other hand, significant advances have been made recently in the understanding of the failure properties of PSA under tension, essentially, thanks to the displacement-controlled probe tests, fitted with optical observation devices.[5–9] Following these advances, Lindner and Maevis[10] have studied the failure over time of acrylic PSA layers loaded to the subcritical stress level that does not cause immediate failure. Interestingly, they found that the failure under low load did not occur by a progressive creep of the adhesive but by the nucleation of cavities and their progressive growth. These results stress the need to understand the failure mechanisms at the microscopic level, before any modeling using the material properties can be attempted.

In this article, we combine the concept of time-dependent failure and that of a shear geometry to investigate *in situ* the failure micromechanisms of PSA, under controlled displacement conditions. The adhesive properties in shear have been investigated using a modified friction device designed to shear the adhesive films between a glass plate and a glass spherical lens at imposed displacement rates. Using the resources of *in-situ* contact visualization, the failure processes have been investigated as a function of the adhesive rheology and the film thickness. To simplify the material parameters, this study focused on two acrylate-based adhesive films differing by their extent of crosslinking. Acrylate-based PSAs present the advantage of being tacky, requiring no additional formulation and also allowing the tuning of the viscoelastic and nonlinear elastic properties through the control of the degree of crosslinking.

EXPERIMENTAL

Thin-Film Elaboration

The shear tests have been performed using two crosslinked adhesive materials elaborated from formulations differing only by the amount of crosslinking agent. In both the cases, the adhesive formulation was a copolymer based on the following monomer composition: 2-ethyl hexyl acrylate (54 wt %), acrylic acid (5 wt %), methyl acrylate (31 wt %), and iso-octyl acrylate (10 wt %). The copolymers were synthesized in solution by UCB Chemicals. Additionally, the solutions contained different amounts of a temperature-activated crosslinking agent. In the subsequent part of this article, acrylate films denoted to as "material A" and "material B" will refer to the adhesives crosslinked using 0.05% and 0.35% of the crosslinking agent, respectively.

The copolymers were provided by UCB as concentrated solutions in a solvent mixture of 54.6 wt % of ethyl acetate, 35.7 wt % of heptane, and 9.7 wt % of isopropanol.

To elaborate the adhesives films, the viscosity of the solution was first adjusted to about 2800 cp compatible with thin-film formation by casting. Then, adhesives films of thicknesses 20, 60, and 100 μm were elaborated by uniform deposition of adequate volumes of the diluted solutions on microscope slides, which were kept on a perfectly horizontal support. The solvents were evaporated at room temperature for 1 h, followed by 30 min at 100 °C under slight depression (800 mbar). For this system and drying procedure, we expect the evaporation to occur before the crosslinking process, since the solvents used are rather volatile. We, therefore, do not expect variations in degree of crosslinking with layer thickness or through the thickness. The thickness of the films was controlled by weighing the specimens at the end of the drying process. The uncertainty associated with this thickness measurement was about 10%.

The glass-transition temperature of the films was found to be −26 °C, using DSC (5 °C/min).

It was not significantly affected by the amount of cross liking agent.

Linear Viscoelastic Measurements

The viscoelastic properties of the adhesives were measured under torsional shear conditions, using a Rheometrics RDA II parallel plates rheometer. Disk specimens nominally 2 mm thick and with a diameter of 8 mm were placed between the two disk plates of the rheometer. Tests have been carried out under isothermal conditions from −30 to 100 °C (*i.e.*, T_g to T_g + 130 °C), using 5 °C temperature steps. Frequencies ranged from 0.1 to 250 rad/s. The strain level was set to 0.5% from −25 to 0 °C, to 1% from 0 to 30 °C and to 5% from 30 to 100 °C. Preliminary strain sweeps have been performed between −25 and 30 °C to ensure that the specimens were strained in their linear range when using such strain levels.

Large Strain Shear Testing

The shear behavior of the adhesives films was investigated using a modified friction device, which operated under imposed displacement conditions. The test geometry was based on a sphere-on-flat contact geometry, in which the adhesive layer was sheared between a flat substrate (the microscope slide) and a glass lens under imposed normal load. The shear device was based on the following main parts (Fig. 1):

i. A moving specimen holder attached to the actuator of a servo-hydraulic testing machine. This holder was fixed to the actuator, using two thin (0.1 mm) steel blades, which ensured a low stiffness in the normal load direction and a high stiffness in the tangential load direction. This arrangement allowed a satisfactory decoupling of the normal and tangential loads. The tangential load, Q, was measured using a 25 N strain gauge transducer (Entran, model ELPM) located below the specimen holder.
ii. A glass lens (radius 9.3 mm) attached to a rigid stationary holder.

The contact normal load was applied by means of a spring located on a linear stage behind the specimen holder. A 50 N strain gauge transducer (Entran, model ELPM) in series with the spring was used to measure the normal load, P.

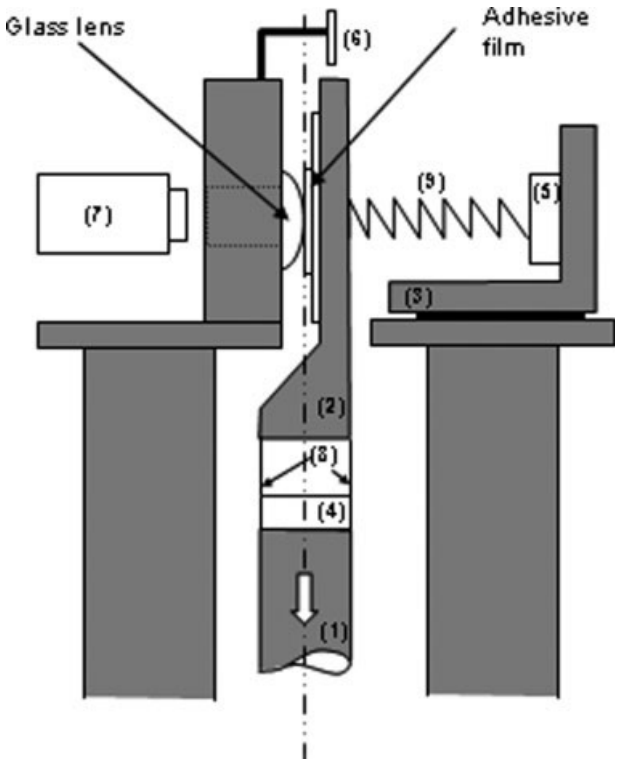

Figure 1. Schematic description of the shear device: (1) rod actuator; (2) specimen holder; (3) linear stage; (4) tangential load transducer; (5) normal load transducer; (6) optical displacement transducer; (7) microscope and CCD camera; (8) leaf springs; (9) spring.

To avoid the transmission of a flexural moment to the load cell during the tangential displacement of the specimen holder, a rotating device (not shown in the figure) was inserted between the spring and the load cell. To ensure a constant normal load during the shear tests, restricting the tangential displacement to a maximum value of 2.0 mm was found necessary.

The relative displacement, d, between the glass lens and the adhesive substrate was recorded using an optical fiberoptic sensor (Philtec model D125), which was located close to the contact area.

During the tests, a microscope equipped with a CCD camera and an image digitalization system allowed the synchronous *in situ* video recording of the contact area during the shearing process to identify the failure mechanism. An image analysis procedure was also developed to determine automatically the changes in the contact area, during the tangential loading.

In the experiments to be described, the normal load was set to 10 N and the displacement rate was fixed at 10 μm/s. Prior to each shear test,

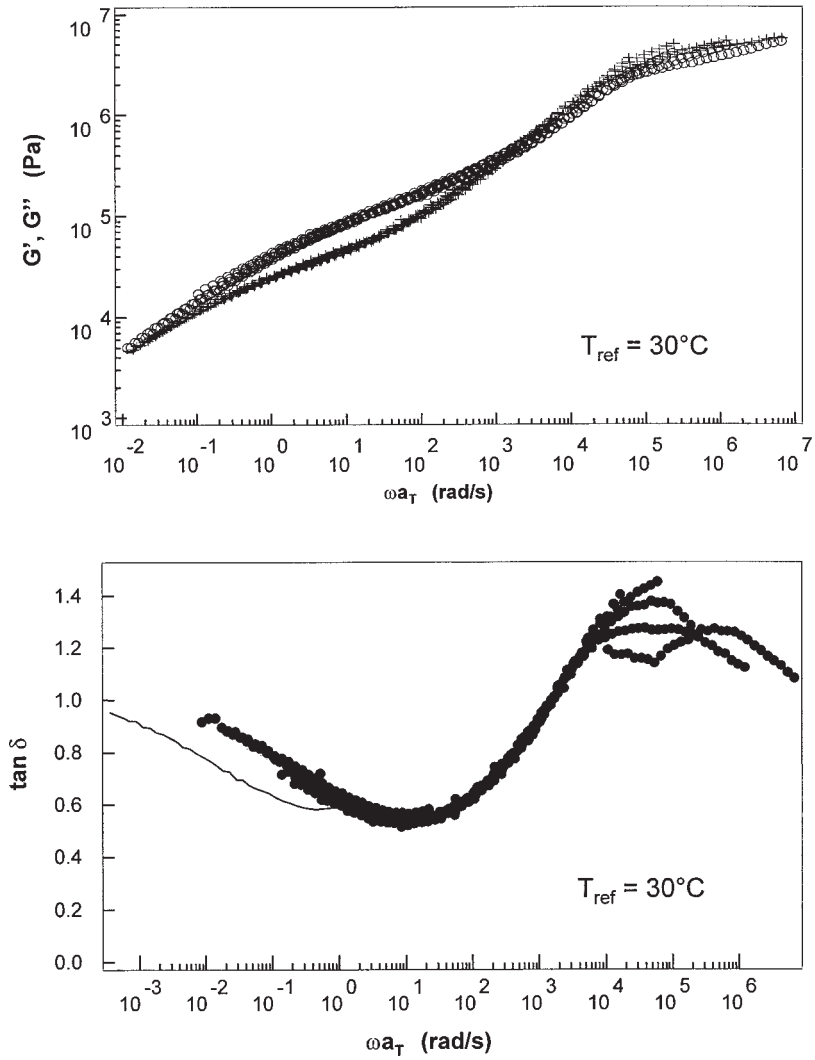

Figure 2. Master curves of the storage modulus (G'), loss modulus (G'') and tangent of the loss angle (tan δ) as a function of reduced frequency for the weakly crosslinked adhesive A, in low-strain oscillatory shear. (○) G'; (+) G''; (●) tan δ.

the glass lens was cleaned in an ultrasonic bath in acetone for 10 min and subsequently dried.

Linear Viscoelastic Behavior

The master curves obtained at 30 °C (Figs. 2 and 3) show that the extent of crosslinking affects significantly the linear viscoelastic properties of the adhesives for frequencies below 1 rad/s.

The lightly crosslinked adhesive (material A) exhibited a polymer melt behavior at low frequencies, which was characterized by a crossover of the G' and G'' curves and a well-defined minimum in tan δ (Fig. 2). On the other hand, material B showed a more elastic-like response in this region, with a higher storage modulus and no clear evidence of a terminal flow region (Fig. 3). At 20 °C and 0.1 rad/s, the real part of the shear modulus of adhesive B ($G' = 220$ kPa) was indeed about ten times that of adhesive A ($G' = 30$ kPa).

All these observations clearly indicate that the increased crosslinking density of material B contributes to the appearance of a more elastic low frequency response under small strain conditions, especially at room temperature.

Large Strain Shear Behavior

Contact Behavior under Normal Loading

A preliminary investigation was carried out to determine the initial size of the contact as a function of the applied normal load and film thickness. The radius, a, of the contact area was

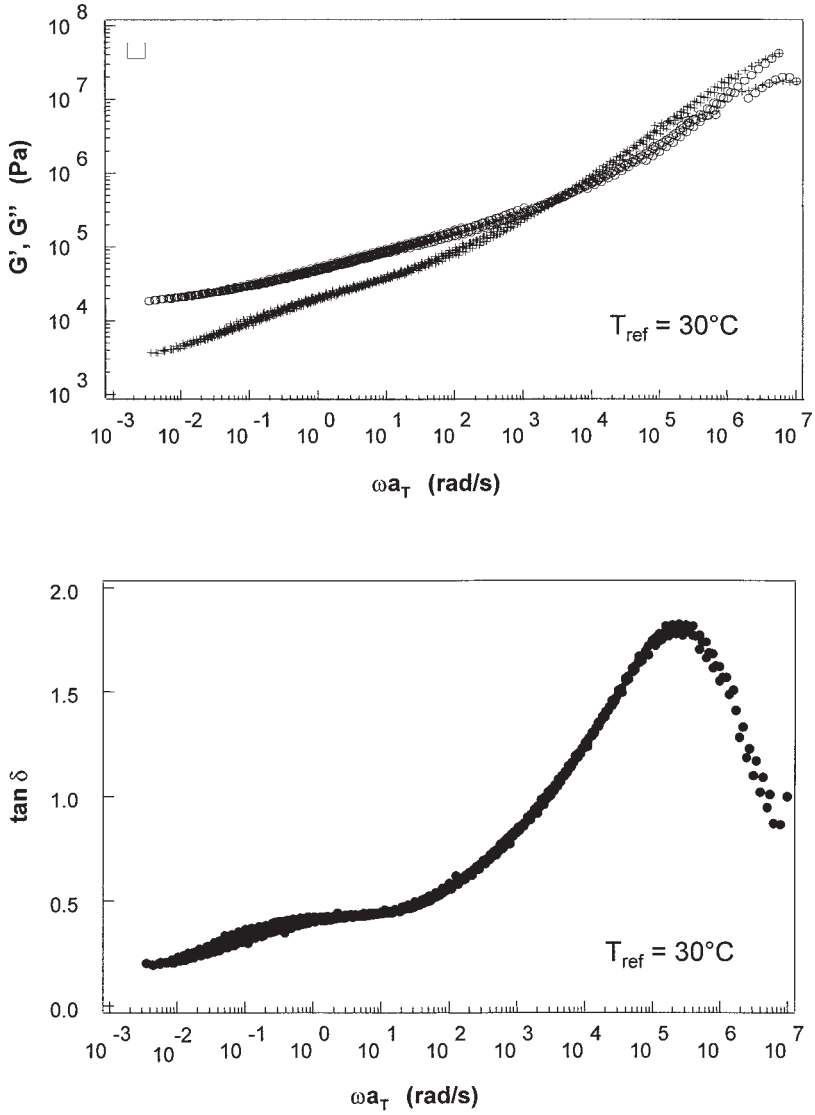

Figure 3. Master curves for the storage modulus (G'), loss modulus (G'') and tangent of the loss angle (tan δ) as a function of reduced frequency for the more crosslinked adhesive B, in low-strain oscillatory shear. (○) G'; (+) G''; (●) tan δ.

measured while increasing the normal load step by step. At each loading step, it was generally observed that the contact size increased slowly as a function of time, as a result of the adhesion kinetics. The data in Figure 4 corresponds to the equilibrium radii measured after stabilization of the contact size, which took place in about 15 min. Although it was not possible to measure a pull-off force, using the present contact device, the adhesive nature of the various contacts is clearly indicated by the finite values of the contact radii at zero load. The contact behavior was also found to be significantly affected by the film thickness and the adhesive properties. For a given film thickness, the lightly crosslinked adhesive (material A) showed larger contact radii than that of adhesive B. Since the surface energy and work of adhesion on glass of these two adhesives are not sensitive to the extent of crosslinking, the increased adhesion of adhesive A to the glass sphere can therefore be attributed to differences in the viscoelastic properties of the materials. As mentioned earlier, the changes in the crosslinking density resulted in a more than 10-fold variation of the low frequency room temperature modulus of the adhesive. As a result, the weakly crosslinked adhesive will present a much higher deformability

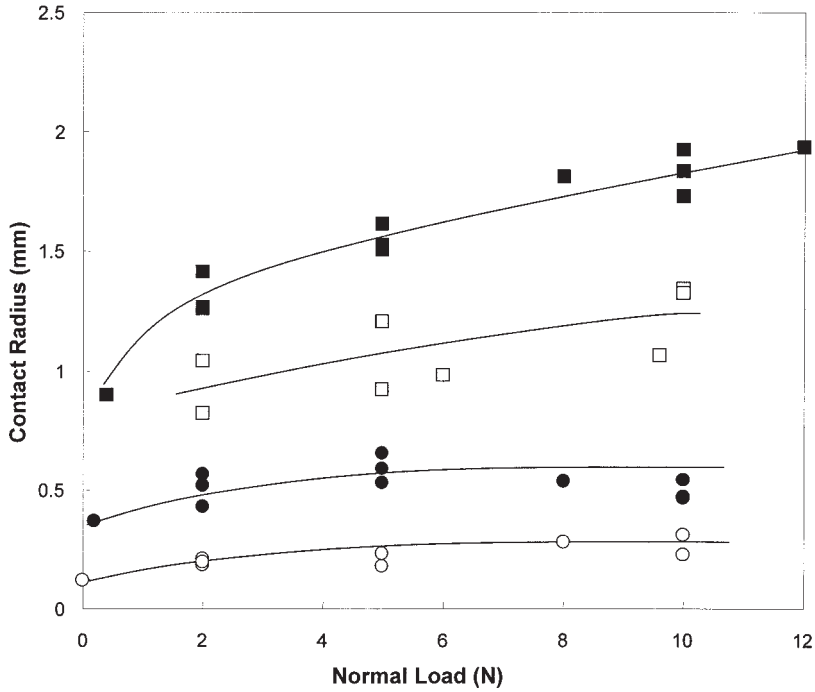

Figure 4. Radius of the adhesive contact as a function of applied normal load and film thickness. (○) adhesive B 20 μm; (□) adhesive B 100 μm; (●) adhesive A 20 μm; (■) adhesive A 100 μm.

within the contact zone under the action of both normal load and surface forces.

A quantitative description of the adhesive behavior of the films for this type of contacts is, however, beyond simple analysis. Some contact mechanics models have been proposed by Shull and coworkers[11,12] to analyze the contact of rigid indenters with soft and incompressible confined adhesive layers. These finite size approaches were, however, validated for moderately confined contact geometries, that is, in situations where the ratio of the contact radius to the film thickness did not exceed 2 or 3. Above these values, the contact behavior becomes highly sensitive to the compressibility of the polymer layer and numerical simulations show that very small fluctuations in the Poisson's ratio of the adhesive close to the rubbery value ($\upsilon = 0.5$) can result in dramatic changes in the compliance of the film.[13–15] Under such conditions, the contact behavior depends on a complex balance between the shear behavior of the layer and its compressibility. In the present experiments, the ratio of the contact radius, a, to the film thickness, h, varied between 5 and 20 depending on film thickness and applied load. An attempt to describe the observed contact behavior using the above models failed to provide realistic values of the contact radii, which demonstrates that the mechanical description of adhesive contacts of confined soft layers is still an outstanding problem.

In-Situ *Visualization of Failure Mechanisms under Steady State Shear*

Weakly Crosslinked Adhesive (Material A). Figure 5 shows a typical example of the failure mechanisms involved during the shearing of a 20 μm thick film of the less-crosslinked adhesive layer (material A) at an imposed displacement rate of 10 μm/s. The applied normal load was 5 N and the nominal shear rate, defined as the ratio of the displacement rate (v) to the film thickness (h), was about 0.5 s^{-1}.

Up to about 400 μm, the tangential load is continuously increased, while *in-situ* contact visualization does not show any significant change in the shape and the size of the contact. Provided that there is no slip at the glass/film interface, this initial stage can thus be related to the bulk shearing of the adhesive layer confined between the two glass surfaces. When the nominal shear deformation exceeded 400 μm, some peeling processes are initiated at the rear edge of the contact. The peeling front shows a distinctive fingering pattern, which is reminiscent of

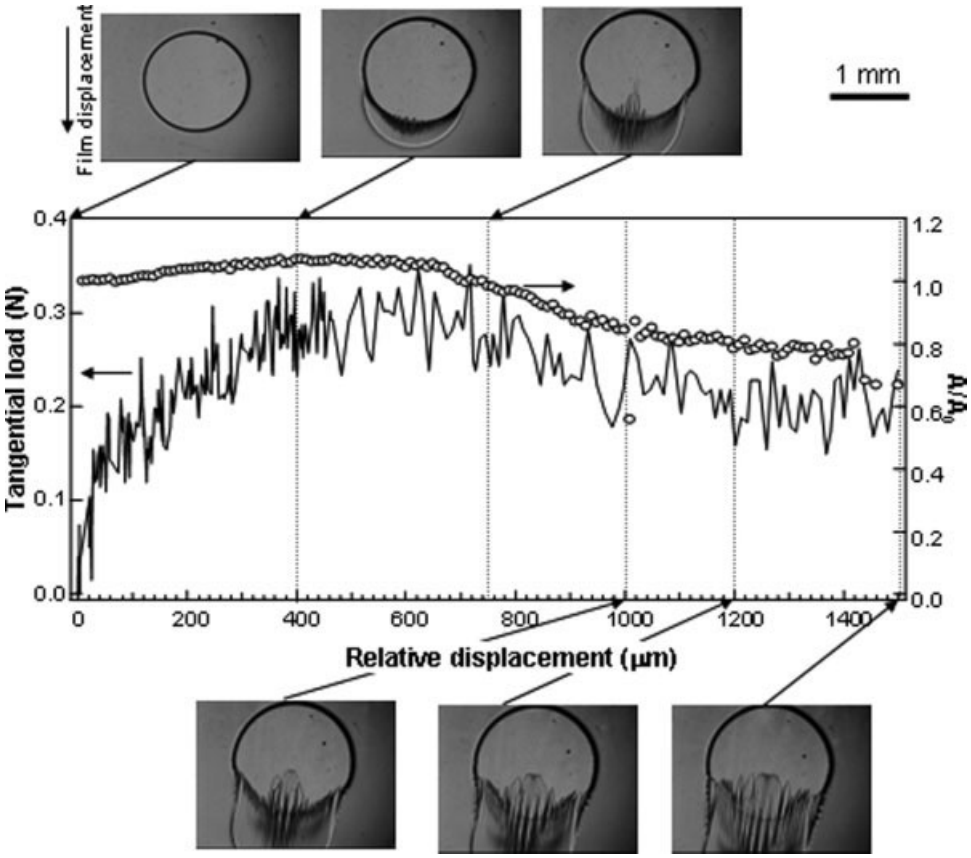

Figure 5. Shear failure mechanisms of a 20 μm thick film of the lightly crosslinked adhesive A. A_0 and A denote the initial and the instantaneous values of the contact area, respectively. (○): relative changes in the contact area, A/A_0; continuous line: tangential load.

Saffman–Taylor instabilities for liquids[16–18] or elastic instabilities for soft solids.[19,20] These fingering instabilities of the peel front are then associated with extensive deformation and orientation of the polymer chains in the direction of the motion of the shear device. This type of deformation is analogous although slightly different to what is observed in 90° peel tests of PSA, described as fibrillation.[21–23] The propagation of the peeling front was associated with only a limited reduction in the tangential load, which could indicate that energy dissipation arises essentially from the deformation and the shear flow of the adhesive film in the nonlinear regime. In that sense, the more-lightly crosslinked adhesive A fails in an essentially cohesive manner.

Similar experiments were also carried out, using thicker adhesives films of material A (h = 60 and 100 μm). Because of the enlarged adhesive contact areas, it proved, however, impossible to initiate significant peeling or debonding processes within the maximum allowed displacement range (up to 2 mm). In other words, the observed behavior was, for practical reasons, restricted to the initial rheological stage associated with the bulk shearing of the adhesive layer within the contact zone.

Highly Crosslinked Adhesive (Material B). Figure 6 shows the failure mechanisms involved during the shearing of a 20 μm thick film of the more crosslinked adhesive layer (material B). Peeling and fibrillation processes similar to that of adhesive A were observed at the rear edge of the contact, during the course of the tangential loading. However, the onset of peeling is associated with a distinct peak of the tangential load, which was not the case for the lightly crosslinked adhesive A. The pictures also show some evidence of the occurrence of detachment waves within the contact, during the initial peeling stages, according to a mechanism

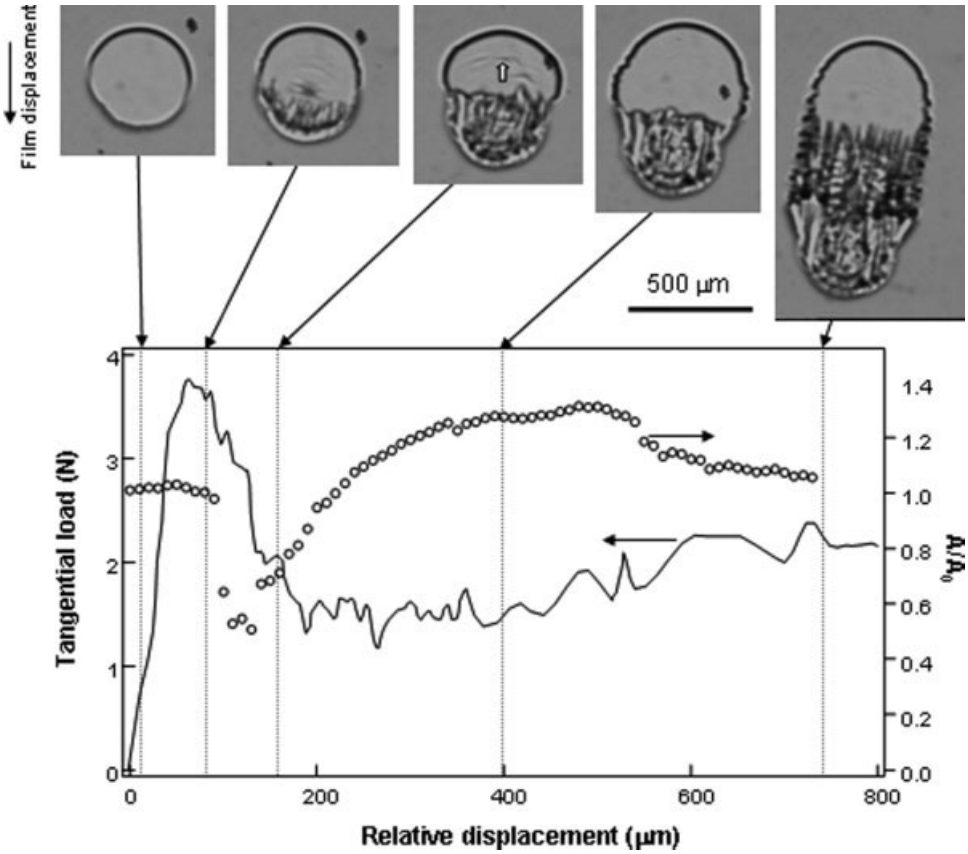

Figure 6. Shear failure mechanisms of a 20 µm thick film of the more crosslinked adhesive B. A_0 and A denote the initial and the instantaneous values of the contact area, respectively. (○): relative changes in the contact area, A/A_0; continuous line: tangential load. The white arrow indicates the occurrence of detachment waves within the contact area.

similar to the generation of Schallamach waves within glass/rubber contacts.[24–26] The associated relative displacement at the interface could account, at least partly, for the observed relaxation of the tangential load. After the load peak, some subsequent increase in the contact area is observed, which results essentially from both the accumulation of the adhesive material at the front edge of the contact and some readhesion of the leading edge of the contact. These readhesion processes are probably enhanced by some elastic recovery of the shear deformation, which could occur as a result of interface slippage.

Similar experiments using thicker films of the more crosslinked adhesive B allowed us to get a more detailed insight into the interactions between the peeling processes and the interface slippage during the shear failure of the adhesive contacts. As an example, Figure 7 shows the different mechanisms involved in the shear failure of a film that is 60 µm in thickness. Three successive stages are identified.

i. A first stage (stage A in Fig. 7) where the initial increase in the tangential load is associated with a slight increase in the contact area, which can be attributed to some pile-up of the adhesive film at the front edge of the contact. This part of the curve corresponds essentially to the bulk shearing of the polymer disk entrapped between the two glass surfaces.
ii. During the second stage (stage B in Fig. 7), the contact area becomes smaller and loses its circular symmetry with a marked shrinkage of the trailing edge. The latter results from the peeling process induced by the tensile stresses at the rear of the contact. As opposed to the 20 µm thick film or less crosslinked adhesive A, a regular peeling front is observed, with no evidence of fingering.

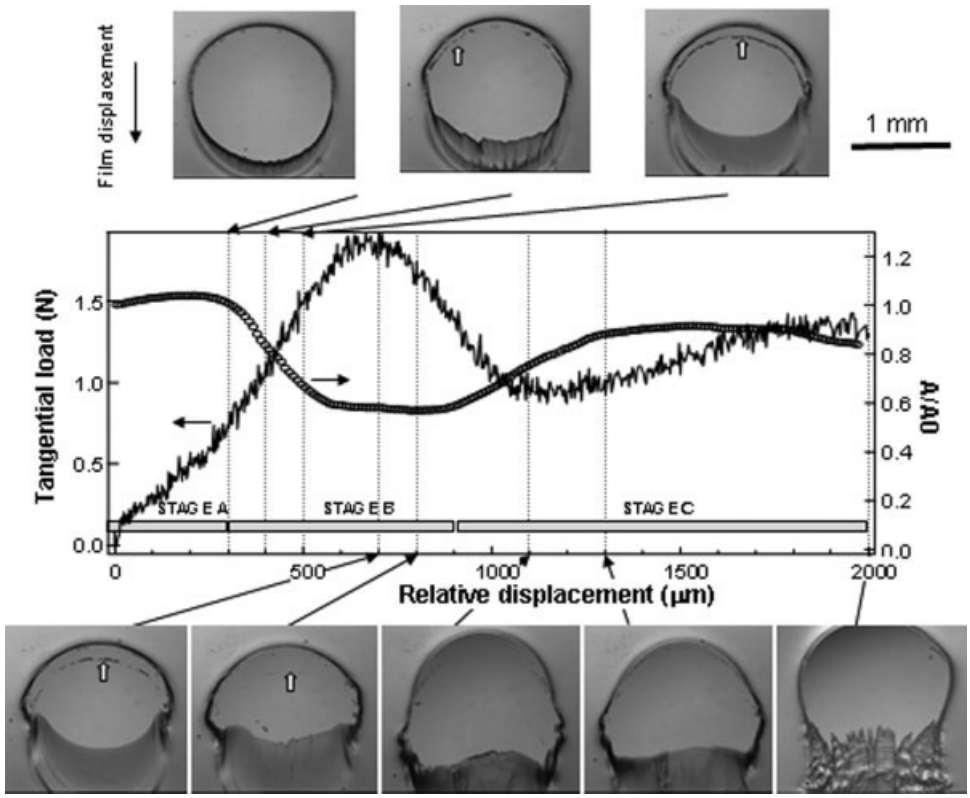

Figure 7. Shear failure mechanisms of a 60 μm thick film of the more crosslinked adhesive B A_0 and A denote the initial and the instantaneous values of the contact area, respectively. (○): relative changes in the contact area, A/A_0; continuous line: tangential force. The white arrows indicate the occurrence of detachment waves within the contact area.

It can be noted that similar peeling processes have already been reported by Barquins in the context of friction experiments in glass/rubber contacts.[27] The peeling front propagates progressively, until the debonded area occupies approximately half of the initial circular contact area. During this stage, the tangential load exhibits a peak value, which can be interpreted by considering the occurrence of two competitive processes: (a) an increase in the tangential load because of the increased shear strain applied to the adhesive part of the contact and (b) a decrease in the tangential load associated with the relaxation of tensile and shear stresses within the peeled part of the contact. The load values obtained during stage B indicate that the first effect predominates until the peak value of the tangential load, that is, during the most important part of the peeling process.

iii. A third stage (stage C), which is characterized by some readhesion of the debonded adhesive film at the rear edge of the contact. Surprisingly, the tangential load is initially decreasing during the first part of this stage (between about 900 and 1100 μm), despite the simultaneous increase in the contact area associated with readhesion. This decrease in the tangential load tends to indicate that some additional relaxation process is taking place within the contact. A potential mechanism could be the development of slip conditions at the interface between the glass sphere and the polymer film. Although it was not possible to identify directly the interface microslip from the *in situ* observation, some observations support this assumption. During stage B, the formation of curved waves of detachment was noted close to the front edge of the contact (as indicated by white arrows in Fig. 7). These waves seemed to result from the formation and the adhesion of buckles close to the contact front edge, in accordance with

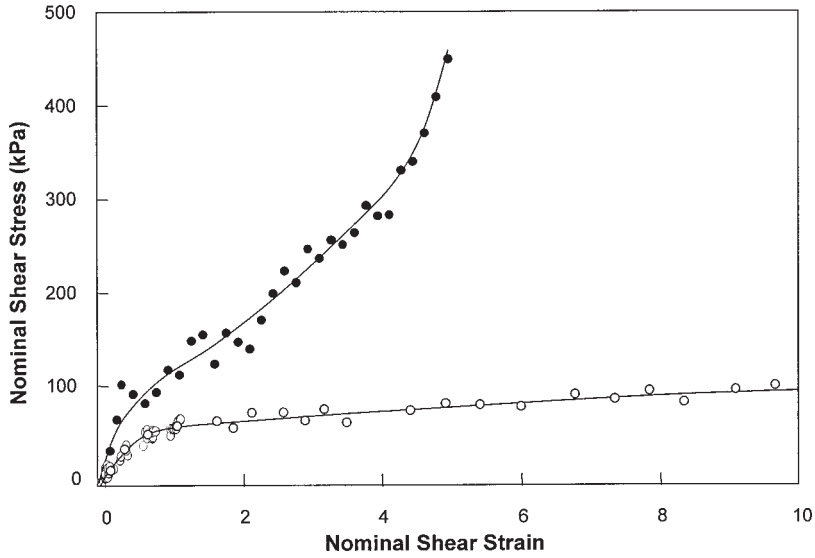

Figure 8. Nominal shear stress as a function of nominal shear strain before the onset of peeling (h = 60 μm, nominal shear rate 0.16 s^{-1}). (○) lightly crosslinked adhesive A; (●) more crosslinked adhesive B.

the generation of Schallamach waves in glass/rubber contacts.[24–26] These detachment waves propagated slowly toward the center of the contact, during stage B. They suddenly disappeared at the beginning of stage C, which could be attributed to some interface relaxation processes resulting from the propagation of slip at the interface.

At the end of stage C, some peeling processes were also found to restart at the rear edge of the contact, according to a mechanism similar to that involved in stage B, but with a more fibrillar nature. This suggest that if very large relative displacements were considered, the failure of the adhesive contact would occur in a stick-slip manner, as a result of the combination of successive peeling and interfacial slippage stages.

As a conclusion, the results for the thicker films (60 and 100 μm) of material B clearly indicate the significant contribution of adhesive mechanisms (peeling and interface slippage) to the failure of the contacts.

RESULTS AND DISCUSSION

Large Strain Rheological Behavior

For both adhesives, it was possible to identify an initial stage characterized by the bulk shear deformation of the circular portion of the film enclosed within the adhesive contact zone, in the absence of any significant peeling mechanisms. Provided that no slip occurs at the glass adhesive/interface, this stage may thus be viewed as a signature of the bulk rheological response of the adhesive material. By virtue of the confinement of the polymer layer, high shear strain values are achieved even under moderate relative displacements, which means that the adhesive is strained far beyond its linear regime. During this stage, a nominal shear stress can be defined by the ratio of the measured tangential load to the instantaneous value of the contact area. Figure 8 shows this nominal shear stress for adhesives A and B, as a function of the nominal strain, as defined by the ratio d/h of the relative displacement to the film thickness. For the lightly crosslinked adhesive, a nearly constant shear stress is achieved quite rapidly, which presents some similarities with the steady shear flow of a liquid-like material. These trends are consistent with the linear viscoelastic results, which also showed that the weakly crosslinked material exhibited a liquid-like behavior in the low strain range. Within this regime, a viscosity can tentatively be calculated from the ratio of the shear stress (about 80 kPa) to the nominal strain rate, v/h, where v is the imposed displacement rate. A viscosity of about 5×10^5 Pa s is obtained, which is close to the values reported by Zosel for similar PSA.[3]

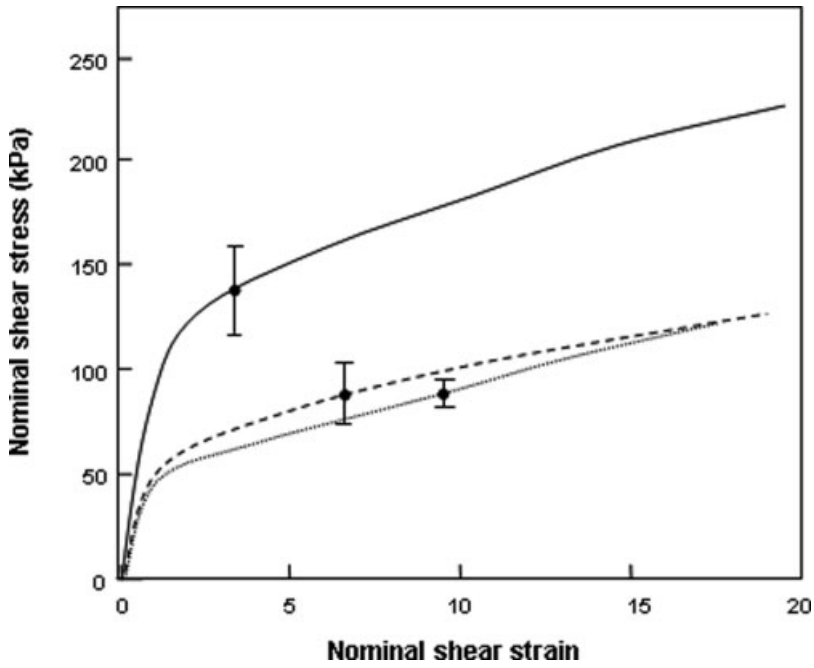

Figure 9. Nominal shear stress as a function of the nominal shear strain for the weakly crosslinked adhesive A before the onset of peeling. Small dotted line: $h = 100$ μm; large dotted line: $h = 60$ μm; continuous line: $h = 20$ μm.

On the other hand, a completely different rheological response was obtained for the more crosslinked adhesive B (Fig. 8). The observed nonlinear behavior is largely consistent with the nonlinear elastic behavior in uniaxial elongation of a crosslinked rubber-like material[28] and has been observed for PSA.[29] Within this regime, the adhesive film can sustain a shear strain equal to about 5 and a shear stress close to 450 kPa before the onset of a contact peeling. Such a large shear strain contains a substantial tensile component and causes a significant degree of orientation of the polymer chains in the direction parallel to the substrate.

Within this rheological regime, changes in the film thickness at constant imposed displacement rates resulted in varying nominal shear rates. As an example, Figure 9 shows the stress/strain relationships of the lightly crosslinked adhesive A, differing in their thicknesses. The nominal shear rate associated with these thicknesses were 0.1 s^{-1} ($h = 100$ μm), 0.16 s^{-1} ($h = 60$ μm), and 0.5 s^{-1} ($h = 20$ μm). The observed increase in the nonlinear behavior at large strain rates is qualitatively consistent with what is usually observed with such adhesive materials under tensile loading.[7]

Peeling Mechanisms

The *in situ* observation of the adhesive contacts indicated that shear failure invariably involves some peeling at the leading edge of the contact under the action of tensile stresses. The exact nature of these peeling processes was, however, found to be dependent upon the rheology of the film and its thickness.

In the case of the 20 μm thick films, the main differences between the two adhesives lies in the shape of the first peak in load observed when the peeling starts. In the case of the more crosslinked material B, the peak is very sharp, whereas only a very broad peak is observed for the less crosslinked adhesive A. A tentative explanation for this difference could stem from the different rheological behavior of the two adhesives in the nonlinear regime. The more elastic response of adhesive B (refer previous section) could allow a more substantial storage of elastic energy during the incipient bulk deformation stages of the shearing process. The subsequent rapid relaxation of this elastic energy during the peeling process could therefore account for the observed decrease in tangential load. On the other hand, the essentially viscous nature of the rheological behavior of the more

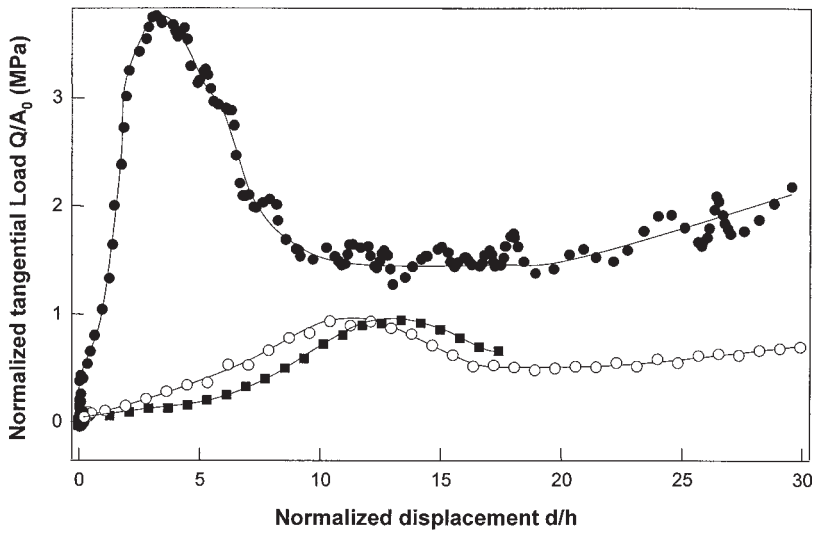

Figure 10. Normalized tangential load, Q/A_0, *versus* normalized displacement, d/h, for the more crosslinked adhesive films (material B). (●) $h = 20$ μm; (○) $h = 60$ μm; (■) $h = 100$ μm.

lightly crosslinked adhesive could prevent the occurrence of such storage/release processes in the case of material A. Another aspect is the direct evidence of some interface slippage in the case of adhesive B, which could also account for the relaxation of the stored elastic energy.

Another interesting aspect of the peeling processes of adhesive B was a much more regular peeling front, associated with distinct detachment waves and interfacial slippage, upon increasing the film thickness up to 60 and 100 μm. At the same time, the confinement of the film (a/h) only increased from 10 to 13, when the film thickness was varied from 20 to 100 μm. From Figure 10, it also appears that the maximum values of the shear stress associated with contact failure are significantly reduced for the adhesives that are 60 and 100 μm in thickness. A first explanation for this transition in the peeling modes could be the sensitivity of peeling and fibrillation processes to the shear rate. In the context of the peeling of uncrosslinked PSA, Verdier and coworkers[22,30] have reported the formation of three-dimensional instabilities in the form of fingers, when the pulling velocity was increased, which are consistent with the present observations: when the film thickness was reduced from 100 to 20 μm while keeping constant the displacement rate ($v = 10$ μm/s), the applied nominal shear rate was increased by a factor of 5, and at the same time, fibrillation was strongly enhanced. Moreover, an examination in the low-displacement regime (*i.e.*, in a region where the shear response is dominated by the bulk film behavior) of the curves reported in Figure 10 provides some indication of a significant sensitivity of the rheological response of material B to strain rate.

Another explanation for these differences in the peeling processes of adhesive B could involve the dependence of the energy release rate on the thickness of the adhesive: peeling indeed remains as an interfacial fracture process, which is sensitive not to stresses but to a critical value of an energy release rate in shear, G_{IIc}. A detailed investigation of this later hypothesis would, however, require an evaluation of the critical energy release rate associated to the peeling processes in the contact geometries under consideration. Such an approach requires extensive contact mechanics calculations taking into account the nonlinear elastic properties of the films, which are beyond the scope of the article.

The observed instabilities in the peel front could be attributed to the increased resistance of the interface to peeling and of the increased strain rate. The peel rate is imposed by the indenter velocity and the adhesive cannot detach fast enough from the interface, with the available elastic energy. As a result, it forms a fingering pattern, which increases its ability to store elastic energy when the speed is increased as discussed for the static case in a recent paper.[19] The appearance of instabilities and the associated fibrillation processes is then a way

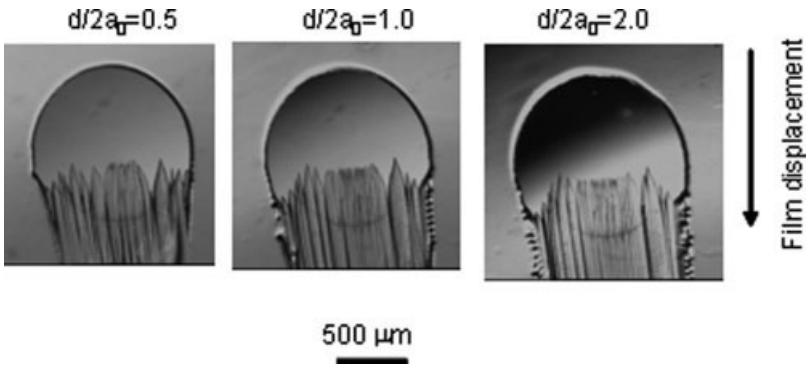

Figure 11. Shear failure mechanisms of the low crosslinked adhesive A under large normalized displacements. d and a_0 are respectively, the displacement and the initial contact radius ($h = 20$ µm).

for the system to increase the stored and released elastic energy necessary to cause the detachment of the fibril at this high speed. Such processes are typically observed for peel tests but can be observed in shear experiments such as ours because of the predominantly tensile loading at the trailing edge of the contact.

The observations also raise some issues regarding the combined effects of peeling processes and interfacial slippage, on the strength of the adhesive films. In the context of the peeling of viscoelastic adhesive, Newby and Chaudhury[31,32] have established that shear stress at the peeling front can be relaxed by a slip process at the interface, which in turn affect the strength of adhesion. In the context of the present shear experiments, it can be noted that the combination of a regular peeling front and interfacial slippage resulted in a strong reduction of the nominal shear strength of the contact, as compared to the 20 µm thick film in which extensive fibrillation and fingering were observed (Fig. 10). This observation tends to indicate that the effects of interfacial slippage on peeling processes can play a significant role in viscoelastic adhesion under both tensile and shear loading.

Sliding Behavior

The experiments with the 20 µm thick PSA films also yield some interesting results regarding the ability of the two glass substrates to slide past each other in the presence of an intercalated adhesive film. As reported earlier, the diameter of the contact area decreases drastically with film thickness. Using the thinnest films, it was therefore possible to induce a tangential displacement exceeding two or three times the diameter of the contact within the maximum prescribed displacement range. Such a situation presents many similarities with the sliding behavior of thin polymer films, where it is known that the frictional behavior is largely dominated by the rheological behavior of the films.[33]

For adhesive B, the peak load associated with the onset of peeling is followed by a stationary regime when the normalized displacement d/h exceeds about 0.5. Under such conditions, the relative displacement between the two glass bodies is accommodated by a combination of fibrillation processes, shear flow, and interfacial sliding (Fig. 6). A coefficient of friction, μ, defined as the ratio of the tangential load to the normal load, can be assigned to these processes. The value, $\mu \approx 0.4$, obtained in the present study is of the order of magnitude of that obtained with glassy or semicrystalline polymer films, where sliding friction involves essentially an interfacial fracture process.

In the case of the lightly crosslinked adhesive A, it was noted that the peeling front at the rear of the contact was stationary with respect to the glass lens (Fig. 11), which suggests that during the sliding stage, energy is rather dissipated by shearing/sliding of the adhesive layer and fibrils extension than by the extension of the peeling front. The associated coefficient of friction, $\mu \approx 0.03$, is intermediate between the values typically obtained with liquid lubricants ($\mu \approx 0.001$) and solid polymer films ($\mu > 0.1$), which supports the idea of a fluid-like behavior of the viscous adhesive within the contact.

As a conclusion, the frictional behavior of the more crosslinked adhesive B seems to be dominated

by highly dissipative interfacial fracture processes, whereas that of the lightly crosslinked adhesive A implies predominantly the shear flow of the polymer film enclosed in the contact zone. These differences are consistent with the data on the large strain rheological behavior of these two adhesives and with the observations of the shear failure mechanisms.

CONCLUSIONS

The shear failure mechanisms of confined adhesive films have been investigated using an original approach based on a sphere-on-flat contact geometry. Using the resources of *in situ* contact visualization, it was possible to identify the shear deformation and failure modes of acrylate adhesive films differing in their rheology and thicknesses, under well-controlled stress conditions.

The initial stages of the tangential loading were found to be associated with the bulk shearing of the adhesive layer in the absence of any significant changes in the shape or size of the adhesive contact. Within this regime, the large shear strains associated with the confined contact conditions allow to get some insight into the large strain nonlinear behavior of the soft adhesive. Significant differences in the shear stress/strain response were indeed observed, when the rheology of the adhesive was changed from liquid-like to rubber-like behavior, by varying the extent of crosslinking. Experiments carried out with films differing in their thicknesses also indicated the possibility of investigating shear rate effects on the rheological behavior.

At large shear strain, failure mechanisms associated with peeling were induced at the rear edge of the contact under the action of surface tensile forces. Depending on the rheological properties of the adhesive, there was also some evidence that these peeling processes were associated with detachment waves and/or slippage at the glass/adhesive interface. Such mechanisms were found to be enhanced in the case of the more crosslinked adhesive, which exhibited a rubber-like behavior. The occurrence of these processes were found to have a pronounced effect on the shear strength of the adhesive films, which extends to shear loading the observations of Newby and Chaudhury,[31,32] regarding the effect of interfacial slippage on the viscoelastic adhesion of adhesive films peeled from a solid substrate. Interestingly, the peeling mechanisms and the associated stress levels change significantly when the layer becomes as thin as 20 μm, which suggests a significant dependence of the energy release rate in shear on the thickness of the adhesive.

The authors thank Steven Van Es at Surface Specialties, for providing the adhesive formulations and financial support. The authors also thank Philippe Sergot for his technical assistance in the design of the shear device. A. Chateauminois is indebted to Arnaud Chiche for stimulating discussions.

NOMENCLATURE

- a Contact radius
- A instantaneous value of the contact area (under shear)
- A_0 initial value of the contact area (under purely normal loading)
- h Film thickness
- P Applied normal load
- Q Tangential load
- v Displacement rate

REFERENCES AND NOTES

1. Creton, C. MRS Bull 2003, 28, 434–439.
2. PSTC. Test methods for pressure sensitive adhesive tapes. Pressure Sensitive Tape Council, 2000.
3. Zosel, A. J Adhes 1994, 44, 1–16.
4. Japanese Industrial Standards, Japanese Standards Association. 2002.
5. Zosel, A. Colloid Polym Sci 1985, 263, 541–553.
6. Lakrout, H.; Sergot, P.; Creton, C. J Adhes 1999, 69, 307–359.
7. Lakrout, H.; Creton, C.; Ahn, D.; Shull, K. R. Macromolecules 2001, 34, 7448–7458.
8. Crosby, A. J.; Shull, K. R.; Lakrout, H.; Creton, C. J Appl Phys 2000, 88, 2956–2966.
9. Brown, K.; Hooker, J. C.; Creton, C. Macromol Mater Eng 2002, 287, 163–179.
10. Lindner, A.; Maevis, T. Langmuir 2004, 20, 9156–9169.
11. Shull, K. R.; Ahn, D.; Chen, W. L.; Flanigan, C. M.; Crosby, A. J. Macromol Chem Phys 1998, 199, 489–511.
12. Shull, K. R. Mater Sci Eng R Rep 2002, 36, 1–45.
13. Creton, C.; Lakrout, H. J Polym Sci Part B: Polym Phys 2000, 38, 965–979.
14. Ganghoffer, J. F.; Gent, A. N. J Adhes 1995, 48, 75–84.

15. Ganghoffer, J. F.; Schultz, J. J Adhes 1996, 55, 285–302.
16. Derks, D.; Lindner, A.; Creton, C. J Appl Phys 2002, 93, 1557–1566.
17. Lindner, A.; Coussot, P.; Bonn, D. Phys Rev Lett 2000, 85, 314–317.
18. Saffman, P. G.; Taylor, G. Proc R Soc London Ser A 1958, 245, 312–329.
19. Shull, K. R.; Flanigan, C. M.; Crosby, A. J. Phys Rev Lett 2000, 84, 3057–3060.
20. Ghatak, A.; Chaudhury, M. J.; Shenoy, V.; Sharma, A. Phys Rev Lett 2000, 85, 4329–4332.
21. Urahama, Y. J Adhes 1989, 31, 47–58.
22. Benyahia, L.; Verdier, C.; Piau, J. M. J Adhes 1997, 62, 45–73.
23. Christensen, S. F.; Everland, H.; Hassager, O.; Almdal, K. Int J Adhesion and Adhesives 1998, 18, 131–137.
24. Barquins, M. Comptes Rendus de l'Académie des Sciences de Paris, Série II 1983, 296, 1567–1570.
25. Koudine, A.; Barquins, M. Comptes Rendus de l'Académie des Sciences de Paris, Série II 1995, 320, 373–379.
26. Schallamach, A. Wear 1971, 17, 301.
27. Barquins, M. Wear 1992, 158, 87–117.
28. Treloar, L. R. G. Rep Prog Phys 1973, 36, 755–826.
29. Ross, A. Ph.D. Dissertation, Ecole Supérieure de Physique et Chimie Industrielles, Paris, 2004.
30. Verdier, C.; Piau, J. M.; Benyahia, L. J Adhes 1998, 68, 93–116.
31. Newby, B. Z.; Chaudhury, M. K. Science 1995, 269, 1407–1409.
32. Newby, B. Z.; Chaudhury, M. K. Langmuir 1997, 13, 1805–1809.
33. Briscoe, B. J.; Smith, A. C. In Reviews on the Deformation Behaviour of Materials, Vol III; Scientific Publications: Israel, 1980; pp 151–191.